

Multiferroicity in the frustrated spinel cuprate GeCu_2O_4

L. Zhao, L. Muzica, U. Schwarz, and A. C. Komarek*

Max-Planck-Institute for Chemical Physics of Solids, 01187 Dresden, Germany

(Dated: April 25, 2022)

Different from other magnetically frustrated spinel systems, GeCu_2O_4 is a strongly tetragonal distorted spinel cuprate in which edge-sharing CuO_2 ribbons are running along alternating directions perpendicular to the c -axis. Here, GeCu_2O_4 samples of high quality were prepared via high pressure synthesis (at 4 GPa) and the corresponding magnetic and dielectric properties were investigated. For the first time, we observed a ferroelectric polarization emerging at $T_N \sim 33$ K. Although the ferroelectric polarization is weak in GeCu_2O_4 ($P \sim 0.2 \mu\text{C}/\text{m}^2$), the existence of spin-induced multiferroicity provides a strong constraint on the possible ground state magnetic structures and/or the corresponding theoretical models of multiferroicity for GeCu_2O_4 .

PACS numbers:

Low dimensional $S = 1/2$ quantum spin systems have been a challenging topic of continued interest within contemporary condensed matter physics. A vast amount of materials with atomic arrangements including quasi two-dimensional (2D) layers based on square lattices, plaquettes, triangular or Kagome lattices, quasi one-dimensional (1D) spin chains or ladders are known to exhibit a wide variety of fascinating quantum phenomena at low temperature [1] such as superconductivity, spin dimerization, Bose-Einstein condensation, quantum spin liquid states and multiferroicity which can be observed in these systems with competing charge, spin, orbital and lattice degrees of freedom.

Transition metal oxides with spinel structure have the general chemical formula AB_2O_4 . These materials have been a playground for theoretical studies on frustrated quantum magnets. The B -ions form a three-dimensional (3D) network of corner-sharing tetrahedra similar to a pyrochlore lattice which gives rise to strong geometrical frustration for antiferromagnetically coupled B -site spins. Theoretically, a ground state of quantum spin liquid can be realized in the ideal isotropic pyrochlore lattice. It is well known that many spinel magnetic compounds exhibit unusual magnetic properties and various ground states with or without long range magnetic ordering. The material-specific details like ion anisotropy and structural distortions are able to lift the high degeneracy [2].

GeCu_2O_4 crystallizes in a strongly distorted spinel structure (Hausmannite) with space group $I4_1/amd$ [3]. The lattice parameters amount to $a = b = 5.593$ Å and $c = 9.396$ Å. GeCu_2O_4 exhibits drastically elongated CuO_6 octahedra in c -direction due to a strong Jahn-Teller effect for the Cu^{2+} ions, see Fig. 1(a). The ab -plane "intra-chain" exchange J in a - or b -direction is much larger than the "inter-chain" exchange J_x in c -direction. From the analysis of its magnetic susceptibility $J_x/J \sim 0.16$ has been reported [4]. The interaction

between chains in the same layer is also weak. The directions of these chains are orthogonal to these lying in the neighboring layers.

Theoretically the real pyrochlore lattice can be simplified by the projection onto a 2D checkerboard pattern known as the planar pyrochlore antiferromagnetic and crossed-chain model (CCM), which conserving the magnetic frustration and interaction anisotropy. In the simple anisotropic limit ($J_x \ll J$) which might be assumed for GeCu_2O_4 a crossed-dimer ground state is predicted [5]. Later, a more detail work combined with density function calculation proposed the ground state of GeCu_2O_4 being a spin spiral state along the chains of edge-sharing CuO_4 plaquettes [6]. The spiral state is common for many quasi-1D frustrated J_1 - J_2 spin chain compounds. Such a spiral magnetic structure is able to induce electric polarization and strong magnetoelectric coupling [7]. However, the calculation [6] predicts an opposite twisting direction for neighboring chains arising from the inter-chain exchange and, thus, no macroscopic polarization.

So far, only a few measurements have been reported on the physical properties of GeCu_2O_4 [4, 8] since the spinel is meta-stable and can only be synthesized at high pressure [3]. In spite of the three-dimensional nature of the spinel structure, a magnetic susceptibility characteristic for a quasi-1D Heisenberg spin $1/2$ chain system with J of ~ 135 K has been reported [4]. Moreover, long range antiferromagnetic ordering emerges below 33 K. Very recently, a powder neutron diffraction experiment [8] reported a novel collinear 'up-up-down-down' ($\uparrow\uparrow\downarrow\downarrow$) pattern along each spin chain within the ab plane, which contradicts previous theoretic predictions [6]. However, also for the experimentally observed magnetic structure [8] no multiferroicity can be expected.

We noticed that the complex structure of GeCu_2O_4 which consists of intertwined quasi-1D CuO_2 spin chains strongly resembles some structural motifs in CuO_2Cl_2 [9]. CuO_2Cl_2 is a newly discovered spin-driven multiferroic material [10] with high transition temperature (~ 70 K). Hence, we synthesized GeCu_2O_4 single crystals at high pressures and analyzed the dielectric and pyroelectric

*Electronic address: Alexander.Komarek@cpfs.mpg.de

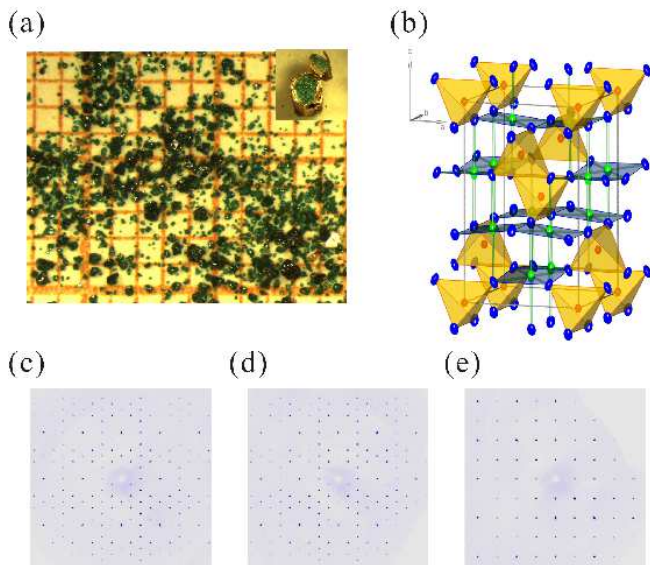


FIG. 1: (a) A photo of our synthesized GeCu_2O_4 single crystals. (b) Representation of the crystal structure of GeCu_2O_4 as obtained from our single crystal X-ray diffraction measurement. The Cu-oxygen plaquettes are indicated by the blue areas; red/green/blue ellipsoids denote Ge, Cu and O ions (99% probability ellipsoids). (c-e) x-ray scattering intensities in the $0KL$, $H0L$ and $HK0$ plane of reciprocal space indicating the single crystalline nature of our GeCu_2O_4 single crystal.

properties of this spinel oxide. Our measurements reveal the unexpected existence of multiferroicity in GeCu_2O_4 questioning the reported models of its magnetic ground state.

First, polycrystalline mixtures were prepared by solid-state reaction. The starting materials of GeO_2 and CuO were mixed in a molar ratio of 1 : 2 and, then, sintered for 50 h at 850°C in air with intermediate grindings. The resulting blue product is composed of GeCuO_3 and CuO as confirmed by powder x-ray diffraction. Next, the obtained powder was sealed in cylindrical gold capsules, which were inserted in a BN sleeve and, then, pressurized with a multi-anvil high pressure apparatus to 4 GPa pressure and, finally, heated to 900°C . After annealing at 900°C for 30 minutes, the sample was cooled to room temperature before the high pressure was released. Quasi-hydrostatic pressures were generated with a Walker-type multi-anvil assembly [11] in combination with a hydraulic press for force generation. For pressure redistribution, we used octahedra manufactured from MgO with 5% Cr_2O_3 and an edge length of 18 mm. Calibration of p , T conditions was performed independently before the experiments. Temperatures were measured with type-C thermocouples and pressures were determined using the resistivity changes of Bi and Pb at room temperature. Within the gold capsule a dense green pillar could be obtained after the high pressure synthesis. This color change from blue to green has also been observed in previous reports of the high pressure synthesis of GeCu_2O_4

atom	x	y	z
Ge1	0	0	0
Cu1	0	1/4	5/8
O1	0	0.24171(9)	0.35882(6)
atom	U_{11} (\AA^2)	U_{22} (\AA^2)	U_{33} (\AA^2)
Ge1	0.00196(3)	0.00196(3)	0.00389(5)
Cu1	0.00273(5)	0.00238(4)	0.00786(5)
O1	0.00367(16)	0.00306(16)	0.00725(15)
atom	U_{12} (\AA^2)	U_{13} (\AA^2)	U_{23} (\AA^2)
Ge1	0	0	0
Cu1	0	0	0.00010(3)
O1	0	0	0.00184(11)
atom	U_{iso} (\AA^2)	occup.	
Ge1	0.00260(2)	1	
Cu1	0.00432(3)	1	
O1	0.00466(9)	1	

TABLE I: Structural parameters derived from the crystal structure refinement of our single crystal X-ray diffraction measurement; $a = 5.5929(4)\text{\AA}$, $c = 9.3984(6)\text{\AA}$, space group: $I4_1/amd$.

[3]. If the dwelling time at 900°C was enhanced and the subsequent cooling rate was decreased, the aggregation of small transparent green single crystals (grown via self-nucleation) of $50\ \mu\text{m}$ to $500\ \mu\text{m}$ size could be observed, see Fig. 1(a).

Powder x-ray diffraction (XRD) measurements have been performed using with $\text{Cu K}\alpha_1$ radiation on a *Bruker D8 Discover A25* powder x-ray diffractometer indicating a single phase of GeCu_2O_4 .

Single-crystal XRD measurements have been performed at room-temperature using $\text{Mo K}\alpha$ radiation on a *Bruker D8 VENTURE* single-crystal x-ray diffractometer equipped with a bent graphite monochromator for about $3\times$ intensity enhancement and a *Photon CMOS* large area detector. An as-grown single crystal with roughly $40\text{-}\mu\text{m}$ diameter has been measured and a multiscan absorption correction has been applied to the data (minimum and maximum transmission: 0.5706 and 0.7536, respectively). For space group $I4_1/amd$ 17773 reflections (H : $13 \rightarrow 10$, K : $12 \rightarrow 14$, and L : $21 \rightarrow 21$) have been collected with an internal R value of 2.71%, a redundancy of 24.0 and 99% (89.7%) coverage up to $2\Theta = 117.7^\circ$ (144.5°). The Goodness of fit, the R- and weighted R-values within the crystal structure refinement amount to 1.63, 1.53% and 4.27% respectively. The structural parameters are listed in Tab. 1 and the obtained crystal structure is plotted in Fig. 1(b). The x-ray scattering intensities within different planes in reciprocal space are shown in Fig. 1(c-e) and indicate the single crystalline nature of our measured crystal.

For the study of the dielectric properties of GeCu_2O_4 , the dense polycrystalline sample was cut and polished to thin plates with thickness of 0.1-0.3 mm. Silver paint was

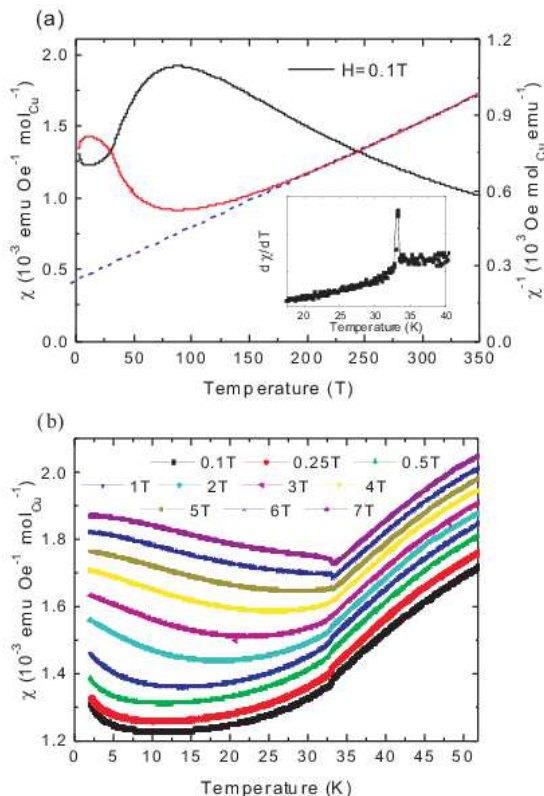


FIG. 2: (a) The temperature dependence of the magnetic susceptibility $\chi(T)$ of GeCu_2O_4 (black) and χ^{-1} (red) measured in an external field H of 0.1 T. The dashed line denotes a Curie-Weiss fit. In the inset the derivative ($d\chi/dT$) is shown. (b) χ measured under different applied fields H ranging from 0.1 T to 7 T. For clarity, all the curves are shifted vertically except for $H = 0.1$ T.

applied to both sides as electrodes to form parallel plate capacitors whose capacitance are proportional to the dielectric constant ϵ . The samples have been mounted on the cryogenic stage and inserted in a *Quantum Design* 9T-PPMS. A high-precision capacitance bridge (*AH 2700A, Andeen-Hagerling Inc.*) was used for dielectric measurements. No apparent difference was observed in the different measuring conditions (various excitation voltages, sweeping rates and integration times have been applied). The electric polarization has been obtained by the pyroelectric current method. First, we polarized the specimens during the cooling process with a static electric field of 1-5 MV/m. Then, we short-circuited both sides of the sample at base temperature for about one hour in order to remove any possible trapped interfacial charge carriers. The pyroelectric current was measured on heating with a heating rate of 3-5 K/min. The electric polarization P has been obtained from the integration of the measured pyroelectric current. Magnetic properties have been measured on a SQUID magnetometer (*MPMS3, Quantum Design Inc.*).

The temperature dependence of the magnetic susceptibility $\chi(T)$ of GeCu_2O_4 measured in a field of 0.1 T is

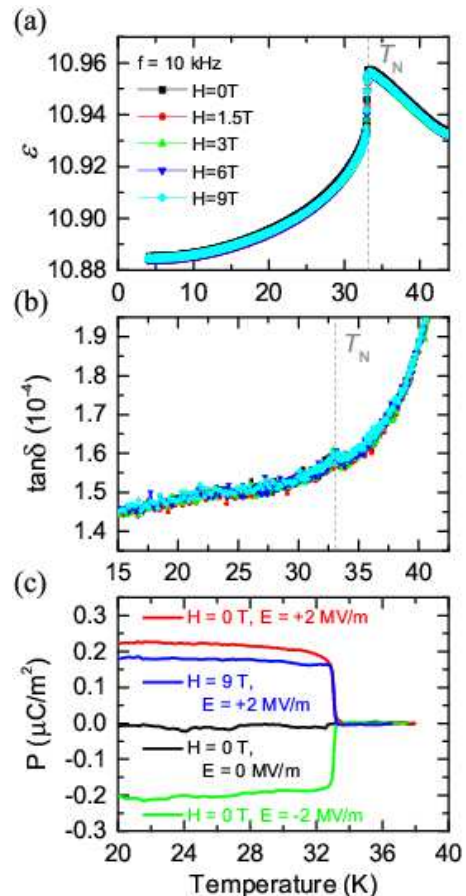


FIG. 3: Temperature dependence of the dielectric constant $\epsilon(T)$ of polycrystalline GeCu_2O_4 under different magnetic fields $H = 0$ T - 9 T. (b) The corresponding tangential loss $\tan\delta$. All these curves have been measured at the frequency of 10 kHz. (c) The temperature dependence of the electric polarization (obtained by integration of the pyroelectric current) which was measured after different poling processes (+2 MV/m, 0 MV/m and -2 MV/m).

shown in Fig. 2(a). Zero-field-cooled (ZFC) and field-cooled (FC) measurements coincide. Around 80 K a broad hump appears which is characteristic for short range antiferromagnetic ordering due to frustration effects. A simple Curie-Weiss fit within the temperature range of 180 K to 350 K yields a Curie-Weiss temperatures θ_{CW} of about -110 K and an effective magnetic moment μ_{eff} which amounts to $\sim 1.94 \mu_B$ which is similar with previous studies [4]. The value of μ_{eff} is slightly higher than that might be expected for the paramagnetic Cu^{2+} spin-only value ($1.73 \mu_B$). At low temperature $\chi(T)$ exhibits a slight drop at $T_N \sim 33$ K suggesting the emergence of long range magnetic ordering. As shown in the inset, the corresponding temperature derivative exhibits a sharp peak at T_N .

We also studied the magnetic field dependence of $\chi(T)$ for different fields up to 7 T. All $\chi(T)$ curves coincide above T_N (including the value of T_N). On cooling below

T_N , the temperature dependence of $\chi(T)$ changes from a decreasing behavior in low fields to an increasing one in high fields above 4 T.

Our results resemble the ones reported in Ref. [8] where $\chi(T)$ was also explained by adding a minor contribution of paramagnetic impurities like GeO_2 . In fact, about 3.6% GeO_2 was found in their samples according to x-ray diffraction. However no such impurities exist in our GeCu_2O_4 samples. (We also measured the magnetic susceptibilities of pure GeO_2 , GeCuO_3 , and CuO powder as reference materials in order to search for possible impurities below the detection level of x-ray diffraction. But, no anomalies can be detected around 33 K for these reference materials, confirming that our observed field evolution of $\chi(T)$ is intrinsic for GeCu_2O_4 .)

The temperature-dependence of the dielectric constant $\epsilon(T)$ measured at a frequency of 10 kHz for different fields H is shown in Fig. 3(a). On cooling ϵ slightly increases for temperatures somewhat above T_N and, then, ϵ drops sharply at the magnetic transition temperature T_N . In our experiments, we also measured ϵ with various frequencies between 1 kHz and 20 kHz (not shown here), and, the observed dielectric anomaly shows no difference for all tested measuring frequencies. This confirms the intrinsic origin of the dielectric anomaly at T_N which -although weak- can also be seen in the corresponding dielectric loss, see Fig. 3(b). As shown in Fig. 3(a-b), the effect of external magnetic fields on the dielectric behavior is almost negligible for the whole studied range of magnetic fields H up to 9 T.

Moreover, we measured also the pyroelectric current in order to study the electric polarization of GeCu_2O_4 . A small but sharp pyroelectric current peak emerges at T_N . The electric polarization in GeCu_2O_4 was obtained by integrating the small pyroelectric currents with our high SNR (Signal Noise Ratio) setup, see Fig. 3(c). To minimize the accumulative error and uncertainty due to noise within the background, the integration was carried out from above T_N to just above 20 K where the polarization has almost saturated (P_s in our notion). Although P_s is quite small -about $0.2 \mu\text{C}/\text{m}^2$ at 20 K- it can be inverted with opposite poling whereas the measured pyroelectric current and corresponding polarization is negligible for zero poling field, see Fig. 3(c). Our observation reveals the weak ferroelectric nature of GeCu_2O_4 below T_N . GeCu_2O_4 , the polarization and magnetoelectric effect is much weaker than in most known multiferroic cuprates as LiCu_2O_2 [16]. However, for the first time, we discovered a new multiferroic material with a strongly tetragonally distorted spinel structure.

The appearance of an ferroelectric polarization at the magnetic ordering temperature is indicative for spin-induced multiferroicity in GeCu_2O_4 . The appearance of an electric polarization that is induced by the magnetic structure has been studied thoroughly for the last decade [12–14]. Three major microscopic origins of spin-induced ferroelectricity are known: (i) exchange-striction arising from the symmetric spin exchange interaction in

certain collinear spin ordering states in some frustrated systems with magnetically inequivalent ions. The "up-up-down-down" spin arrangement along the atomically alternating A-B spin chains observed in $\text{Ca}_3(\text{Co,Mn})\text{O}_6$ [15] is an example for this first mechanism; (ii) the Inverse Dzyaloshinskii-Moriya (DM) or spin current model. Via spin-orbit interaction two non-collinear magnetic moments are able to induce a local electric polarization $\mathbf{P}_{ij} = A\hat{\mathbf{e}}_{ij} \times (\mathbf{S}_i \times \mathbf{S}_j)$ with ($\hat{\mathbf{e}}_{ij}$ being the unit vector between the two sites i and j .); and (iii) the Arima model where the spin-dependent p - d hybridization induces a local polarization $P_{il} \propto (\mathbf{S}_i \cdot \hat{\mathbf{e}}_{il})^2 \hat{\mathbf{e}}_{il}$ with ($\hat{\mathbf{e}}_{il}$ being the unit vector connecting magnetic ion and ligand site. The last two models (ii) and (iii) require certain magnetic and/or lattice structure such that the sum over the crystal lattice sites is not canceled out and such that a non-zero macroscopic polarization P emerges. Model (ii) is able to yield non-zero P e.g. for cycloidal magnetic structures [16] whereas model (III) requires a certain Bravais lattice that hosts e.g. a screw-type helical magnetic structure [17]. For both models (ii) and (iii) the magnitude of the induced polarization P usually rather weak.

In GeCu_2O_4 the presence of identical magnetic ions -i.e. Cu^{2+} ions- excludes the possibility of mechanism (i). The lattice symmetry (space group $I4_1/\text{amd}$) also excludes the possibility of the last mechanism (iii). For the spiral magnetic ground state that was theoretically predicted [6] the spins are spiraling along each chain with the renormalized pitch angle of about 84° . But, the induced polarization cancels out due to opposite twisting directions in neighboring chains. Also for the cross-dimer state [5] no polarization P can be expected since this dimer ground states does not break inversion symmetry. For example, GeCuO_3 is such a spin-dimer system where no dielectric anomaly could be observed at T_N [18]. So far, there is only one reported neutron diffraction measurement on a GeCu_2O_4 powder sample [8]. The experimentally measured collinear "up-up-down-down" spin structure is also centrosymmetric and incompatible with emergence of spin-induced multiferroicity. Hence, further studies on its spin structure based on high quality powder samples or single crystals are necessary for an understanding of the mechanism of multiferroicity in GeCu_2O_4 .

Conclusively, in this work, we presented magnetic, dielectric and polarization measurements on the metastable GeCu_2O_4 spinel oxide prepared by high pressure synthesis. We observed spin-induced ferroelectricity in GeCu_2O_4 , where all the experimentally or theoretically proposed spin structures are not compatible with existing theoretical models for multiferroicity (or vice versa). Due to the complex intertwining of quasi-1D CuO_2 spin chains and strong inherent frustration effects within the tetragonally distorted spinel structure, interesting physics can be expected as an outcome of future theoretical and experimental studies on this new multiferroic material.

Acknowledgments

We would like to thank R. Castillo for the support in the sample preparation. We also would like to thank

L. H. Tjeng for his support and for helpful discussions. The research is partially supported by the Deutsche Forschungsgemeinschaft through SFB 1143 and through DFG project number 320571839.

-
- [1] U. Schollwöck, J. Richter, D.J.J. Farnell, and R.F. Bishop, R.F. Quantum Magnetism, Springer (2004)
 - [2] H. Takagi and S. Niitaka, Introduction to Frustrated Magnetism, chapter 7, 155, Springer (2010).
 - [3] W. Hegenbart, F. Rau and K.-J. Range, Mat. Res. Bull. **16**, 413 (1981).
 - [4] T. Yamada, Z. Hiroi, M. Takano, M. Nohara, and H. Takagi, J. Phys. Soc. Jpn. 69, 1477 (2000).
 - [5] O. A. Starykh, A. Furusaki, and L. Balents, Phys. Rev. B **72**, 094416 (2005).
 - [6] A. A. Tsirlin, R. Zinke, J. Richter, and H. Rosner, Phys. Rev. B **83**, 104415 (2011).
 - [7] Y. Tokura, and S. Seki, Adv. Mater. **22**, 1554 (2010)
 - [8] T. Zou, Y.-Q. Cai, C. R. dela Cruz, V. O. Garlea, S. D. Mahanti, J.-G. Cheng, and X. Ke, Phys. Rev. B **94**, 214406 (2016).
 - [9] S. V. Krivovichev, S. K. Filatov, and P. C. Burns, Can. Mineral. **40**, 1185 (2002).
 - [10] L. Zhao, M.T. Fernández-Díaz, L.H. Tjeng and A.C. Komarek, Sci. Adv. **2**, e1600353(2016).
 - [11] D. Walker, M. A. Carpenter and C. M. Hitch, Am. Mineral. **75** 1020 (1990).
 - [12] S.-W. Cheong and M. Mostovoy, Nat. Mater. **6** 13 (2007)
 - [13] Y. Tokura, S. Seki, and N. Nagaosa, Rep. Prog. Phys. **77** 076501 (2014)
 - [14] K.F. Wang, J.-M. Liu, and Z.F. Ren, Adv. Phys. **58** 321 (2009)
 - [15] Y. J. Choi, H. T. Yi, S. Lee, Q. Huang, V. Kiryukhin, and S.-W. Cheong, Phys. Rev. Lett. **100**, 047601 (2008).
 - [16] S. Park, Y. J. Choi, C. L. Zhang, and S.-W. Cheong, Phys. Rev. Lett. **98**, 057601 (2007).
 - [17] T. Arima, J. Phys. Soc. Jpn. **76**, 073702 (2007).
 - [18] Y. Tsunazumi, N. Ogita, J. Akimitsu, E. Nakamura, and M. Udagawa, J. Phys. Soc. Jpn. **65**,3404 (1996).